JOURNAL OF Applied Polymer SCIENCE

Poly(ether imide)-Modified Benzoxazine Blends: Influences of Phase Separation and Hydrogen Bonding Interactions on the Curing Reaction

Pei Zhao, Xiaomin Liang, Jie Chen, Qichao Ran, Yi Gu

State Key Laboratory of Polymer Materials Engineering, College of Polymer Sciences and Engineering, Sichuan University, Sichuan, Chengdu 610065, China

Correspondence to: Q. Ran (E-mail: qichaoran@126.com) or Y. Gu (E-mail: guyi@scu.edu.cn)

ABSTRACT: Polymer blends of polybenzoxazine (PBZ)/poly(ether imide) (PEI) were prepared by the *in situ* curing reaction of benzoxazine (BZ) resin in the presence of PEI. Phase separation induced by the polymerization of BZ resin was observed. The rheological behaviors, morphologies, and their evolution process of BZ/PEI blends were investigated by rheometer and scanning electron microscope. Phase separation that took place at the early stage of the curing reaction effectively reduced the dilution effect of PEI. Fourier transform infrared (FTIR) results suggested that hydrogen bonds between PBZ and PEI existed during the whole curing process, although weakened with phase separation. The decrease of isoconversion activation energy indicated that the polymerization of BZ resin was facilitated in the presence of such kind of hydrogen-bonding interactions. By changing the weight fraction of PEI, extensive phase separation was obtained in PBZ blends with 5 and 20 wt % of PEI, in which systems, the crosslinking density and glass transition temperature (T_g) of PBZ-rich phase were greatly improved compared to this single PBZ system. © 2012 Wiley Periodicals, Inc. J. Appl. Polym. Sci. 000: 000–000, 2012

KEYWORDS: thermosets; thermoplastics; morphology; hydrogen bonding; curing of polymer; glass transition temperature

Received 5 May 2012; accepted 9 August 2012; published online
DOI: 10.1002/app.38459

INTRODUCTION

Because of its excellent thermal and mechanical properties, flame retardancy, and versatility in molecular design, polybenzoxazine (PBZ) has been widely used in the field of high-performance composite materials.[1–5] Different with other thermosetting (TS) resins such as epoxy, cyanate ester, and bismaleimide resins, PBZ has a lot of intramolecular or intermolecular hydrogen bonds (H-bonds) [Scheme 1(a, b)],[6] which endow PBZ with amazing properties, such as high glass transition temperature (T_g), high modulus, and low moisture absorption.[1,3,5,7–10] However, these H-bonds on the other hand can increase the rigidity of the segments during the curing process and hinder the polymerization of benzoxazine (BZ) resin, leading to the lower chemical crosslinking density,[9,11] which is disadvantageous to the improvement of the property of PBZ resin. So, how to increase the crosslinking density of PBZ without sacrificing its hydrogen bonding interactions is significant to further improve its properties, especially T_g.

In fact, introducing external H-bond donors or acceptors into the PBZ system to compete with the native H-bonds of PBZ can improve the mobility of BZ segment during the curing process, thus finally can enhance the crosslinking density of PBZ. Ishida and Lee[12] have prepared PBZ composite with increased crosslinking density by blending with polycaprolactone (PCL). Because the carbonyl groups of PCL could form intermolecular H-bonds with the phenol groups of PBZ, the native hydrogen bonding interactions of PBZ were attenuated, and the mobility of BZ segment was enhanced, which facilitated the polymerization of BZ resin.[12] However, the T_g did not improve with the increase in the crosslinking density of PBZ/PCL blends.[13] This phenomenon might be attributed to the plasticization effect of PCL modifiers, caused by the good compatibility between PCL and PBZ.[13]

As for TS/thermoplastic (TP) blending system, an important aspect that should be considered is the influences of dilution and plasticization effect of TP resin on the TS resin. For example, the TP may act as the plasticizer to decrease the T_g of the blends.[13,14] Meanwhile, the polymerization of TS resin can be inhibited by the dilution effects of TP resin. Varley et al.[15] and Mackinnon et al.[16] found that the Arrhenius activation energy ($E\alpha$) and gelation time of TS resin both increased with the increase in the TP content, and they attributed this phenomenon to the dilution effects of TP resin. Nevertheless, considering the change of microstructure of blending system during the

Additional Supporting Information may be found in the online version of this article.

Applied Polymer SCIENCE

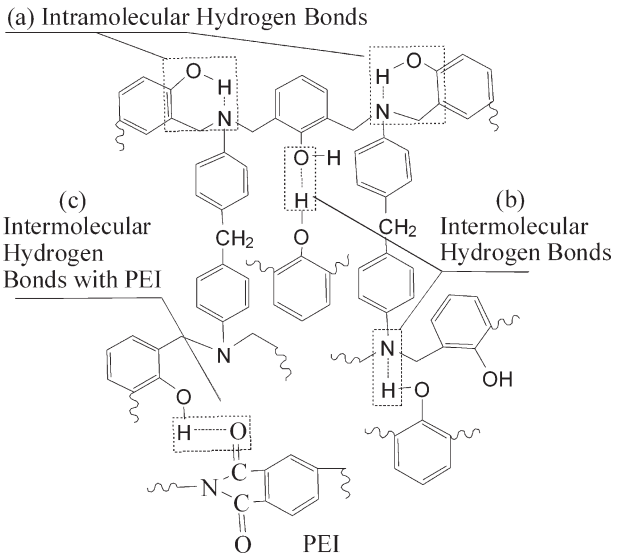

Scheme 1 . H-bonds that could possibly occur in the blends of PEI and PBZ: (a) intramolecular H-bonds between hydroxyl group and nitrogen atom on the Mannich bridge via six-membered ring, (b) intermolecular H-bonds between hydroxyl group and hydroxyl group or hydroxyl group and nitrogen atom on the Mannich bridge, and (c) intermolecular H-bonds between the carbonyl group of PEI and hydroxyl group of PBZ.

TS curing, the dilution and plasticization effect of TP resin may be reduced by choosing proper TP modifier. For example, reaction-induced phase separation would take place in TS/TP blends during the curing process if the thermodynamic difference between TS and TP resin is large enough.[17–20] In this case, TP resins may gradually separate from TS matrix before the occurrence of chemical gelation of TS resin, leading to the decrease of TP content in TS-rich phase.[20,21] Therefore, the dilution and plasticization effect of TP resin on the TS curing can be reduced effectively,[22] and the extent of reduction depends on the competition between the kinetics of phase separation and cross-linking reaction.[15,21]

In this study, poly(ether imide) (PEI), a kind of high-performance engineering TP resin-containing polar groups, was chosen as a H-bond acceptors to modify PBZ, which was expected to form intermolecular H-bonds with PBZ and to improve the polymerization extent of PBZ. Besides, reaction-induced phase separation was designed to reduce the dilution effect of PEI on the curing reaction of BZ resin, because the large thermodynamic difference between PEI and PBZ, which can be reflected by the relative large value of Flory–Huggins interaction parameter (χ) (0.9657, $T = 297$ K) caculated by Flory–Huggins theory and Hildebrand formula,[23,24] is beneficial to phase separation. Rheometer, scanning electron microscope (SEM), Fourier transform infrared (FTIR), differential scanning calorimetry (DSC), and dynamic mechanical thermal analysis (DMA) were used to study the relationship among the phase separation, H-bonding interactions, and curing reaction of BZ resin. This research would help us to further realize the influences of morphological structure and curing reaction on the properties of TP-modified PBZ resin system.

EXPERIMENTAL

Materials

4,4′-Bis(3,4-dihydro-2 H-1, 3-benzoxazin-3-yl)phenyl methane (B-BZ) resin based on 4,4'-diaminodiphenyl methane (DDM), phenol, and paraformaldehyde was synthesized and characterized as previous reports[25] with the cyclic ratio of 87%. Phenol, DDM, and paraformaldehyde were purchased commercially from Chengdu Kelong Chemical Reagents Corp. (China) and used as received. Poly(ether imide) (PEI; Ultem 1000, $M_n = 2.3 \times 10^4$ g/mol, $M_w = 4.0 \times 10^4$ g/mol, $n = 1.7$) was supplied by General Electric Company. The chemical structures of B-BZ and PEI were shown in Scheme 2.

Preparation of B-BZ/PEI Blends

Herein, B-BZ resin was used without further purification. B-BZ/PEI blends with different mass ratios were prepared by mixing PEI and B-BZ in dichloromethane (CH_2Cl_2) at room temperature till a yellow transparent solution was obtained. After filtrating with glass yarn and removing most of the solvent using a rotary evaporator under a reduced pressure at 80°C, the solution was poured into a preheated mold at 140°C and degassed for 45 min under vacuum to remove the residual solvent and trapped air. The curing schedules were used as follows: 140°C/2 h + 160°C/2 h + 180°C/2 h + 200°C/2 h.

B-BZ/PEI blends with 5, 15, and 20 wt % of PEI were named as BP5, BP15, and BP20, respectively. Samples at certain curing stage were signed as $T_{cure} - t$. Herein, T_{cure} and t represented the final curing temperature and curing time, respectively. For example, 180°C–1 h: 140°C/2 h + 160°C/2 h + 180°C/1 h.

Measurements

DSC (TA Q20) was used to determine the conversion of B-BZ resin in each system at different cure stages. The enthalpy was measured with the heating rate of 10°C/min from 40 to 350°C under nitrogen atmosphere. The conversion of B-BZ (α_{BZ}) was calculated from the formula: $\alpha_{BZ} = 1 - H_t/H_0$, where H_t is the residual enthalpy at certain stage and H_0 is the total heat flow of the uncured B-BZ/PEI blending system. What is more, ramp scanning with different heating rates (2, 5, 10, and 20°C/min) under N_2 atmosphere was done to investigate the apparent cure activation energy ($E\alpha$).

The morphologies of the blends with various cure extents were studied by SEM (Philip XL-30 FEG). Samples were fractured under cryogenic conditions, and the fractured surfaces were coated with gold before SEM measurement.

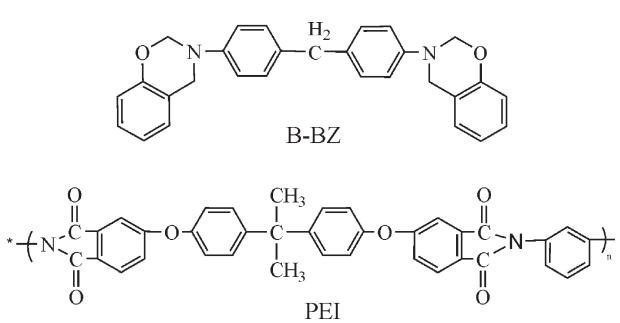

Scheme 2. Chemical structures of B-BZ and PEI.

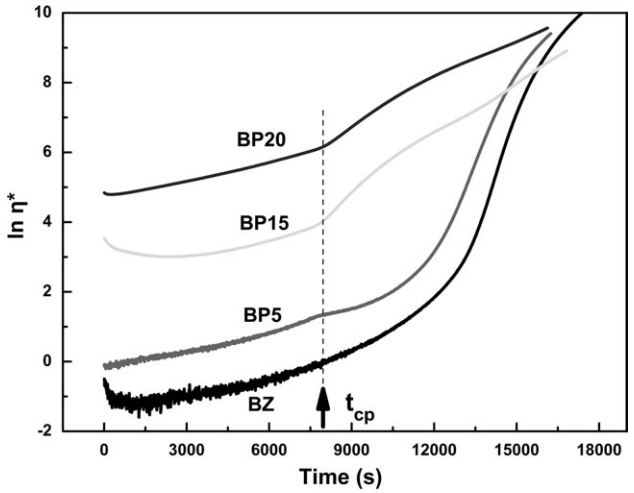

Figure 1. Rheological behaviors of systems with different PEI contents at 140°C.

The isothermal rheological behaviors of the blends were recorded in an Ares-9 A rheometry instrument. About 1 g of the blend was sandwiched between two round fixtures and softened at 120°C for 1 min. The plate distance was then adjusted to about 1.5 mm, and the temperature was raised quickly to 140°C. All the blends were tested under a parallel plate mode with a controlled strain of 1% and test frequency of 1 Hz to ensure that measurements were performed under linear viscoelastic region.

FTIR measurements were performed on Nicolet Magna 560 FTIR spectrometer equipment. Samples for off-line FTIR were prepared by KBr pellets, and samples for in-line FTIR were prepared by dissolving the uncured blend in methylene chloride (CH_2Cl_2) and then casting onto KBr windows. In-line FTIR was performed under the following condition: first, ramp 10°C/min from 10 to 180°C, isothermal holding for 30 min; then ramp 10°C/min from 180 to 200°C, isothermal holding for another 10 min. All the spectra were obtained at a resolution of 4 cm^{-1} and the average of 32 scans.

DMA was performed with a TA Q800 equipment. Specimens with the dimension of 30 × 10 × 3 mm^3 were tested in three-point bend mode. The maximum strain amplitude was 20 μm, and the oscillating frequency was 1 Hz, as the temperature was scanned from 40 to 300°C with the heating rate of 5°C/min. In this study, the peak temperature (T_{peak}) of tan δ is considered as glass transition temperature (T_g). Samples for DMA measurement were cured at 140°C/2 h + 160°C/2 h + 180°C/2 h + 200°C/2 h and then postcured at 210°C/1 h.

RESULT AND DISCUSSION

Rheology and Morphology

Before the curing reaction, all the blends were miscible and presented a transparent yellow color at the temperature range of 0–140°C. With the curing reaction, the initial transparent blends gradually became opaque, implying the occurrence of phase separation induced by the polymerization of B-BZ resin.

The morphological evolution of B-BZ/PEI blends with different PEI content and curing extent was observed by SEM, and the corresponding T_g and conversion of B-BZ were determined by DMA, DSC, and rheological measurements, respectively. Meanwhile, chemical gelation was estimated by observing the solubility of sample at different curing stage in CH_2Cl_2 at room temperature. In all the SEM imagines, the dark region represents PB-BZ-rich phase, and the bright region represents PEI-rich phase. The component of matrix and dispersed phases was obtained based on the isothermal rheological behavior of B-BZ/PEI blends at 140°C.

As shown in Figure 1, the complex viscosity of B-BZ system increased with curing time smoothly due to the increase in molecular weight of B-BZ resin. For B-BZ/PEI systems, when phase separation occurred, the viscosity-raising rate for BP5 system was reduced, while that for BP15 and BP20 system was accelerated abruptly. Bonnet et al.[20] and Blanco et al.[26,27] had observed similar fluctuation in TP-modified TS resin systems at the point of phase separation. Meanwhile, they claimed that the decrease of viscosity or viscosity-raising rate indicated the formation of TP dispersed-rich phase due to the separation of high-viscosity TP resin from TS matrix; while the increase of viscosity or viscosity-raising rate indicated the formation of TP continuous-rich phase due to the separation of low-viscosity TS resin from TP matrix. According to the earlier analysis, in BP5 system, high-viscous PEI formed dispersed phases; while in BP15 and BP20 systems, PEI formed continuous phase.

The morphology of BP5 system was shown in Figure 2. After curing at 140°C for 2 h (α_{BZ} = 15%), small indistinct PEI particles (about 200 nm), which were uniformly dispersed in B-BZ matrix [Figure 2(a)], were observed. This could be seen as "nucleation." Subsequently, more and more PEI molecules gradually separated and accumulated to form larger particles [600–650 nm, Figure 2(b)] till the chemical gelation occurred. Finally, sea-island structure, where global PEI-rich phase evenly dispersed in the PB-BZ-rich continuous phase, was observed in BP5 system [Figure 2(c)].

As shown in Figure 3, the morphology evolution of BP15 system was complicated. After curing at 140°C for 100 min (α_{BZ} = 10%),

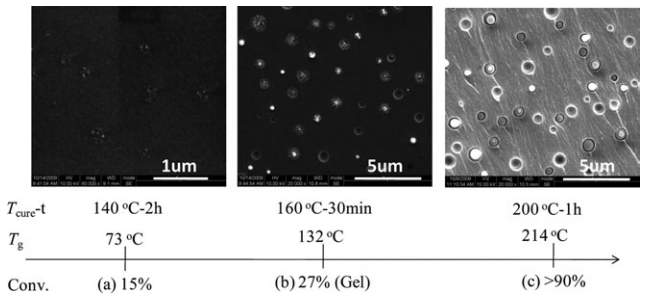

Figure 2. The morpholoy and related B-BZ conversion for BP5 systems. Conversion (α_{BZ}) and T_g were obtained by DSC and DMA measurements; chemical gelation was estimated by observing the solubility of sample in CH_2Cl_2 at room temperature. The original DSC exothermic curves and DMA results were displayed in Supporting Information Figures S1(a) and S2(a).

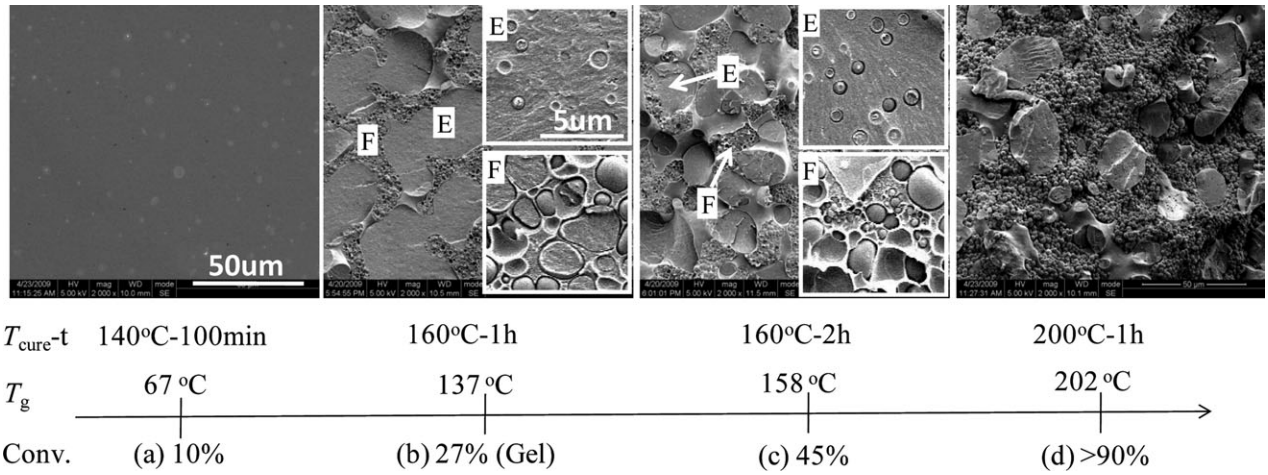

Figure 3. The morpholoy and related B-BZ conversion for BP15 systems. The higher magnifications at two different locations, the B-BZ primary-rich phase (E) and PEI primary phase (F), were shown. Sample of stage (d) were etched by CH_2Cl_2 before SEM observation. The original DSC exothermic curves and DMA results were displayed in Supporting Information Figures S1(b) and S2(b).

primary phase separation was observed [Figure 3(a)]. With the curing reaction, both primary phases grew rapidly, and the increased quench depth promoted the occurrence of secondary phase separation in each primary phase [Figure 3(b)]. That is to say, in primary PEI-rich phase [Figure 3(b-F)], B-BZ oligomers gradually separated from PEI matrix and locally concentrated to form PB-BZ-rich nodules; while in primary PB-BZ-rich phase [Figure 3(b-E)], dispersed PEI particles with the size of 0.5–1.0 μm were observed. After curing at 160°C for 2 h (stage c), some new subparticles were observed in primary PEI-rich phases [Figure 3(c-F)], while no distinct changes were observed in PB-BZ primary phases [Figure 3(c-E)] because of the occurrence of chemical gelation at stage b. Finally, a dual-phase structure, where sea-island structure and phase inversion structure coexisted, was obtained in BP15 system [Figure 3(d)]. Such morphology has been reported in PCL[28] or poly(ether sulfone)[27,29]-modified bisphenol A diglycidyl ether epoxy resin systems.

The morphology evolution process of BP20 system was shown in Figure 4. After curing at 140°C for 75 min (α_{BZ} = 4%), clear phase-inverted structure, where dispersed PB-BZ-rich phase was surrounded with continual PEI matrix, was observed [Figure 4(b)]. With the increase in the conversion of B-BZ resin, more and more B-BZ oligomers were separated from the PEI-rich phase and coalesced with each other to form larger PB-BZ-rich nodules from 0.46 (α_{BZ} = 4%) to 1.59 μm (α_{BZ} = 21%). From then on, the phase separation in PB-BZ-rich particles was terminated by chemical gelation, while the phase separation in PEI-rich phase was undisturbed, and some new nanosized PB-BZ-rich particles, which locally inserted in the PEI-rich phase [Figure 4(d-F)], were observed.

According to the morphology evolution process, when the conversion of B-BZ resin was low, phase separation occurred in all the three B-BZ/PEI blending systems, and PEI molecules were gradually excluded from B-BZ matrix; thus, the dilution effect of PEI on the curing reaction of B-BZ resin was reduced. Clarke

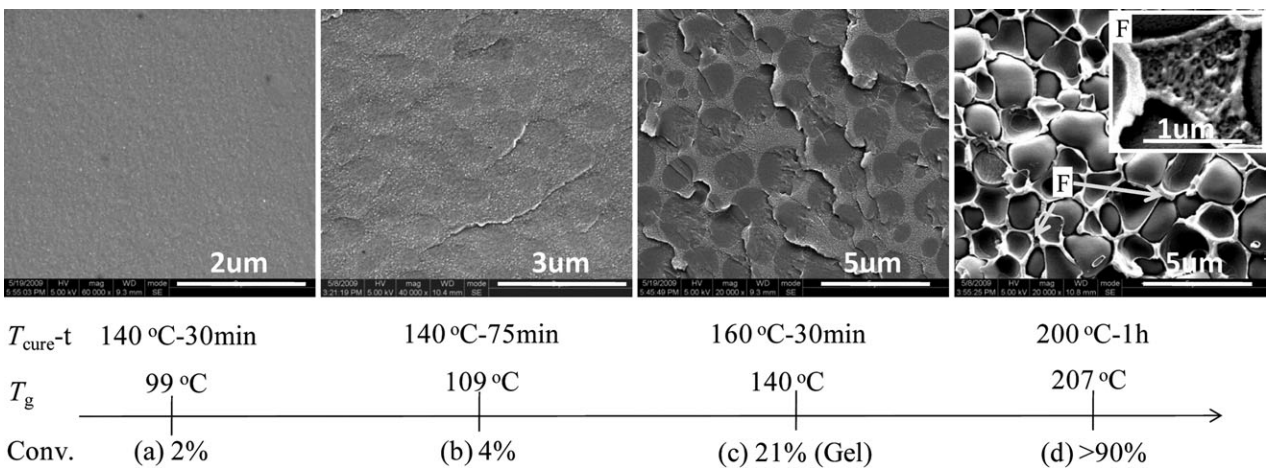

Figure 4. The morpholoy and related B-BZ conversion for BP20 systems. The higher magnification of PEI-rich phase (F) was shown. The original DSC exothermic curves and DMA results were displayed in Supporting Information Figures S1(c) and S2(c).

et al.[30] reported that dual-phase structure is the typical behavior of a blend that undergoes its first separation in the critical region of its phase diagram. For TS/TP blend system at critical composition, it is common that large amounts of TP resin or TS resin still exist in primary TS-rich phase or primary TP-rich phase, respectively.[28–30] In our systems, dual-phase structure was observed in BP15 system, which implied the poor phase separation. Thus, when phase separation occurred, the dilution effect of PEI was more serious in BP15 system than in BP5 and BP20 system.

Hydrogen-Bonding Interactions

In B-BZ/PEI blends, the carbonyl of PEI is expected to form intermolecular H-bonds with phenolic hydroxyl groups produced by ring-opening polymerization of B-BZ resin. Kumar et al.[31] have reported such kind of H-bonds in homogeneous PB-BZ/bismaleimide blends. However, intermolecular H-bonds between TS and TP resin may decrease with the process of phase separation.[12,32] To clarify the existence of such H-bonds, the symmetrical (1778 cm^{-1}) and asymmetrical (1724 cm^{-1}) stretching vibrations of the carbonyl ($\nu_{(C=O)}$) of BP20 system with different curing stage were investigated as an example [Figure 5(a)]. Meanwhile, a new parameter $\Delta\sigma$ ($\Delta\sigma = \sigma_0 - \sigma_c$, where σ_c is the wavenumber of the carbonyl group at specific curing stage and σ_0 is the wavenumber of the carbonyl group in uncured sample) was introduced to quantitatively analyze the shift of carbonyl groups as shown in Figure 5(b).

Before curing reaction (stage b), $\nu_{(C=O)}$ was similar to that of the pure PEI for the lacking of phenolic hydroxyl groups ($\Delta\sigma = 0$). As the curing reaction goes on, more and more phenolic hydrogen groups were produced by the ring-opening polymerization of B-BZ resin; thus, the $\nu_{(C=O)}$ gradually shifted to lower wavenumber (stage b-c-d), indicating the formation of H-bonds between PB-BZ and PEI. After curing at 140°C for 120 min (stage d), $\Delta\sigma$ of symmetrical and asymmetrical $\nu_{(C=O)}$ increased to 2.9 and 2.1, respectively. A similar smaller shift has been reported in polybenzimidazoles/PEI system,[33,34] which was also attributed to the formation of intermolecular H-bonds. From then on, the $\nu_{(C=O)}$ gradually returned to the initial position (stages d–f) and $\Delta\sigma$ almost reduced to zero after curing at 200°C for 1 h (stage f). That was because the increase in molecular weight of B-BZ resin reduced the compatibility between PEI and B-BZ resin and promoted the growing B-BZ precursor to separate from the PEI-rich phases, the opportunity of PB-BZ and PEI collided with each other was reduced.

To verify that the H-bonds between PEI and PB-BZ did not disappear at the end of phase separation (stage f), FTIR spectra of separated PEI-rich phases and PB-BZ-rich phases were investigated. As shown in Figure 4(d), phase-inverted structure was obtained in BP20 system after curing at 200°C for 1 h. Therefore, when the sample of this stage was dipped in CH_2Cl_2 for 24 h, two rich phases were completely separated. PB-BZ-rich phases were insoluble in CH_2Cl_2, and yellow powders were obtained after drying in vacuum. PEI-rich phases were soluble in CH_2Cl_2, and white powders were obtained after precipitating the solution against ethanol and drying in vacuum for 5 h. The FTIR spectra of these two powder samples as well as the pure

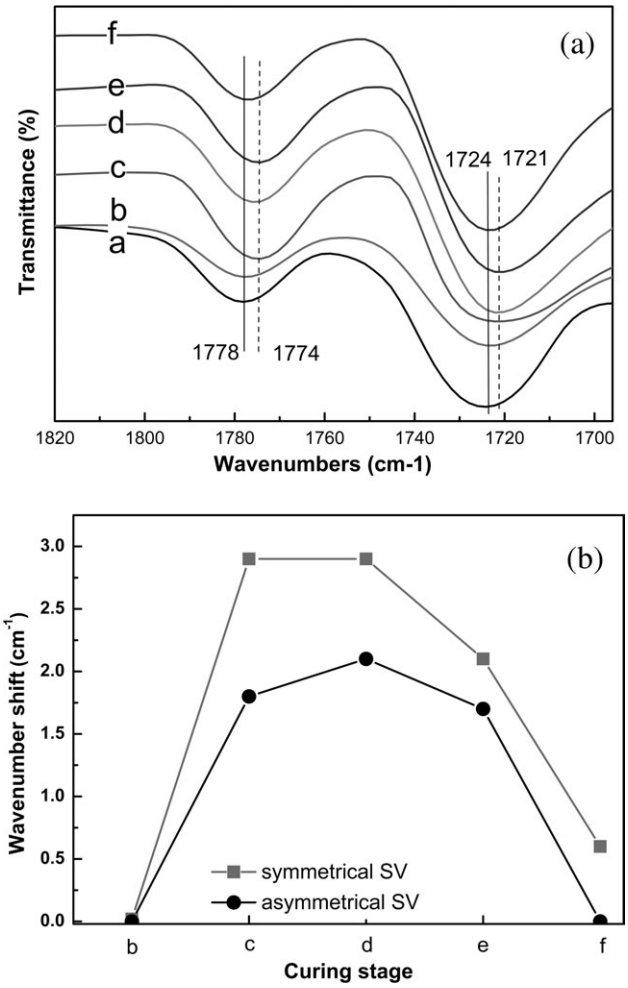

Figure 5. A: FTIR spectra of asymmetrical and symmetrical $\nu_{(C=O)}$ for PEI (a) and BP20 system at different cure stage; (B) $\Delta\sigma$ of carbonyl group at different curing stage: (b) 0 min; (c) 140°C–70 min; (d) 140°C–120 min; (e) 160°C–30 min; (f) 200°C–60 min.

PEI were shown in Figure 6. Interestingly, the shifts of $\nu_{(C=O)}$ almost disappeared in the separated PEI-rich phase, while obvious shift was observed ($\Delta\sigma = 4$ cm^{-1}) in the separated PB-BZ-rich phase. That is to say, the shift of $\nu_{(C=O)}$ in highly cured BP20 system [Figure 5(f)] was not really disappeared, but was concealed by the absorption of nonbonded carbonyl groups in PEI-rich phase.

It is well known that hydrogen-bonding interaction is sensitive to temperature.[3] The intermolecular hydrogen-bonding interactions could be significantly reduced at the elevated temperature (viz. the curing condition) if the intermolecular hydrogen-bonding interactions were not sufficiently strong.[3] In our systems, the H-bond between PEI and PB-BZ was expected to compete with the native H-bonds of PB-BZ during the curing process, but whether such kind of H-bonds [Scheme 1(c)] was stable at curing temperatures was unclear. To make sure of that, in-line FTIR experiment of BP20 blend was done. As shown in Figure 7(a), the asymmetrical $\nu_{(C=O)}$ at 1720 cm^{-1} shifted to higher wavenumber with the elevated temperature. To determine the fraction of H-bonded carbonyl at each stage, the expanded

Applied Polymer SCIENCE

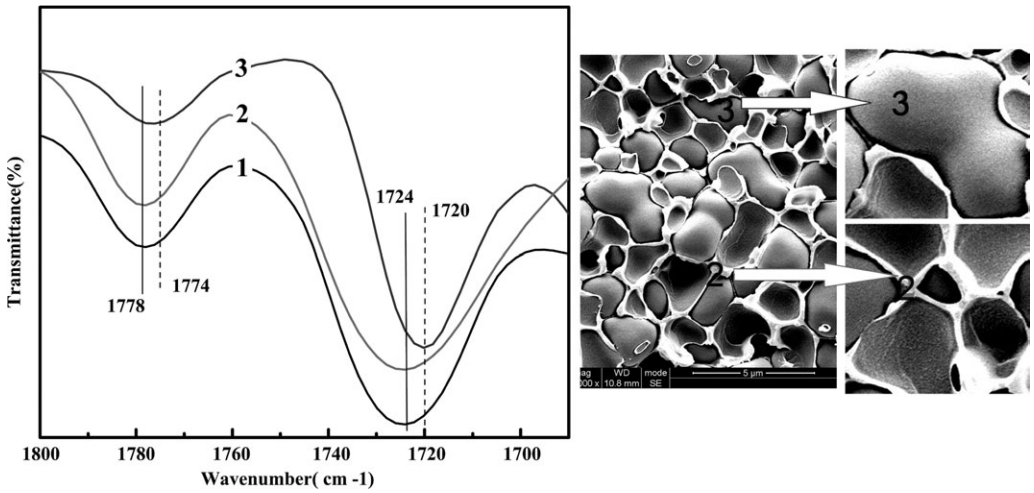

Figure 6. FTIR spectra of asymmetrical and symmetrical $\nu_{(C=O)}$ for pure PEI (1); PEI-rich phase (2), and PB-BZ-rich phase (3) of highly cured BP20 system. (Right: the morphology related to the fully cured BP20 system obtained by SEM).

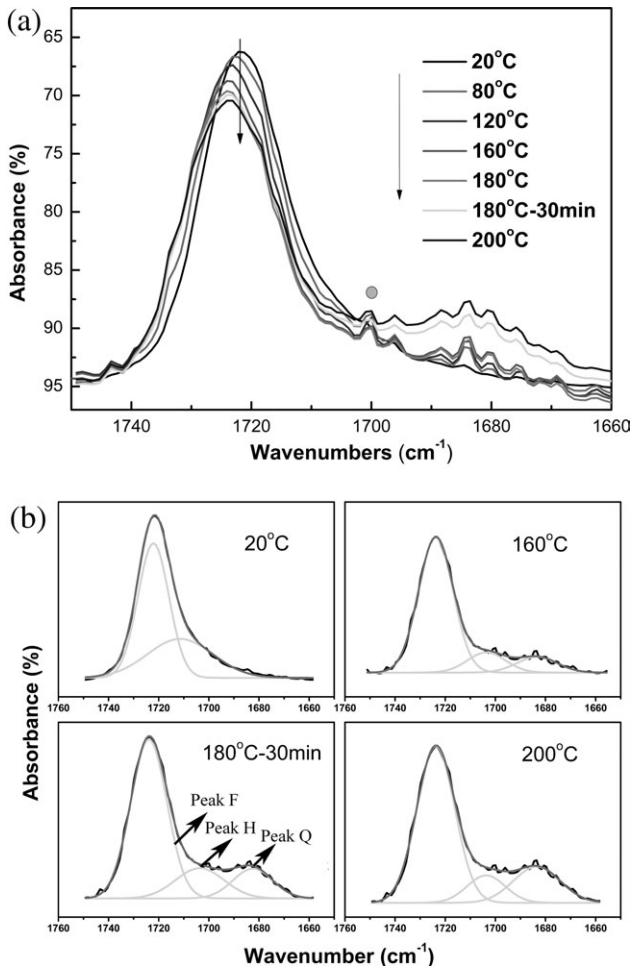

Figure 7. (a) In-line FTIR spectra of asymmetrical $\nu_{(C=O)}$ for BP20 system at different scanning temperatures; (b) fitting curve of in-line FTIR data of BP20 system. (Peak F centered at 1723 cm^{-1} representing the non-bonded carbonyl group; peak H around 1710 cm^{-1} representing H-bonded carbonyl group; peak Q at 1683 cm^{-1} corresponding to quinone-like structure owing to the oxidation of phenolic hydroxyl groups at elevated temperature.[35])

FTIR spectra (1750–1660 cm^{-1}) for BP20 system at different scanning temperatures were fitted by three Gaussian functions via Origin Program 8.0. The results were illustrated in Figure 7(b) and summarized in Table I.

At low temperatures ($T < 120°C$), the area fraction of H-bonded carbonyl (R_H) was about 37%, for the B-BZ resin used here was unpurified. However, when the temperature increased to 160°C, R_H sharply reduced to 14.1%. That is because the occurrence of phase separation induced by the curing reaction of B-BZ resin, reduced the possibility of the formation of hydrogen bonds between PEI and PBZ. Meanwhile, quinone-like structure was observed, which consumed the only H-bond donor of the blend.[35] From then on, the R_H smoothly increased to 20% after curing at 180°C for 30 min due to the increased number of hydroxyl groups. Further increasing the curing temperature, more quinone-like structures were obtained, which further reduced the amounts of H-bonded carbonyl groups. Even so, 15% of R_H was still left at 200°C, which apparently indicated that the H-bonds between PEI and PB-BZ were stable at elevated temperatures.

In summary, it can be concluded that the H-bonds between the carbonyl of PEI and the phenolic hydroxyl groups of PB-BZ [Scheme 1(c)] exist during the whole polymerization process and increase with curing reaction, while decrease with phase separation and the oxidation of phenolic hydroxyl groups.

Curing Reaction

In the blend systems, the electron negativity of carbonyl of PEI is higher than that of the nitrogen atoms on the Mannich bridge of PB-BZ. Meanwhile, phenolic hydroxyl groups produced by the ring-opening polymerization of B-BZ resin were the only H donors. So, the existence of H-bonds between PEI and PB-BZ to some extent could reduce the native H-bonds of PB-BZ. Supposing the exchanges of H-bonds between PEI and PB-BZ [Scheme 1(c)] with the rigid intramolecular H-bonds via a six-membered ring [Scheme 1(a)] of PB-BZ increased the mobility of B-BZ segmental, the curing reaction of B-BZ resin

Table I. Area Fraction of H-Bonded Carbonyl (R_H) of BP20 Blends at Different Scanning Stage

Sample	A_F[a]	A_H[b]	A_Q[c]	$R_H = A_H/(A_F + A_H)$	R^2[d]
20°C	364.6	221.9	0	0.378	0.9992
80°C	413.0	189.0	0	0.313	0.9965
120°C	428.0	234.1	0	0.353	0.9958
160°C	478.0	78.6	64.6	0.141	0.9978
180°C	467.2	88.6	82.0	0.159	0.9970
180°C-10 min	452.5	105.3	84.9	0.189	0.9980
180°C-30 min	444.1	112.9	91.1	0.203	0.9984
200°C	456.6	80.0	130.5	0.150	0.9973

[a]The relative area of free carbonyl, [b]The relative area of H-bonded carbonyl, [c]The relative area of quinone-like structure, [d]Correlation coefficient.

should become easier in the presence of PEI.[12] To certify this hypothesis, the curing behaviors of B-BZ resin and B-BZ/PEI blends were investigated.

According to the theory of molecular collision, apparent reaction activation energy ($E\alpha$) is the comprehensive expression of some parameters, such as concentration, viscosity, and reaction activity of functional groups, which may influence the curing behavior. In this work, $E\alpha$ was used to quantitatively characterize the curing behavior of B-BZ resin and B-BZ/PEI blends. Based on the data of nonisothermal DSC scans at different heating rates (Supporting Information Figure S3), the $E\alpha$ of different conversion ($10\% \leq \alpha_{BZ} \leq 90\%$) was calculated by the Ozawa's isoconversional formula[36] expressed as eq. (1):

$$\ln v = C - 1.052 \times \frac{Ea}{RT_a} \quad (1)$$

where R is the gas constant, C is a constant independent of $E\alpha$, and T_α is the absolute temperature (K) at certain conversion, which can be obtained directly from the integral of the DSC curves at different heating rates (v). The plots of ln v versus $1/T_\alpha$ were shown in Figure 8. The good linear relationships were obtained for B-BZ and B-BZ/PEI blends at different conversions, indicating the validity of Ozawa approach, and thus the activation energy values at different conversions were calculated from the slopes of the plots, as shown in Figure 9.

It is well known that the introduction of high-molecular weight TP resin (modifier) could reduce the diffusion of TS resin due to the high viscosity and dilution effect, thus resulting in higher $E\alpha$ values and lower reaction rates.[22,37–39] In our systems, when

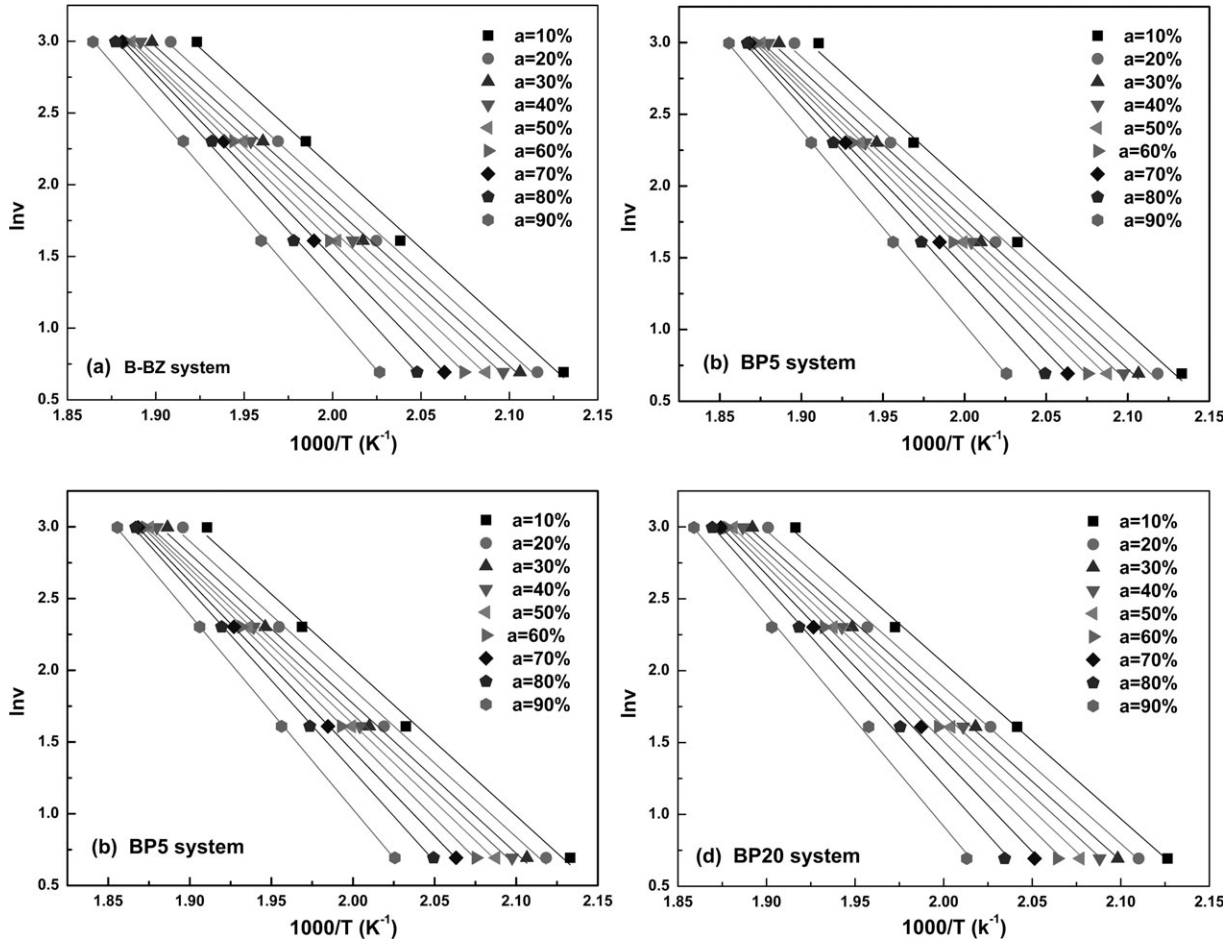

Figure 8. Plots of ln v versus $1000/T$ at different conversions according to Ozawa's iso-conversional method for B-BZ and B-BZ/PEI blend systems.

Applied Polymer SCIENCE

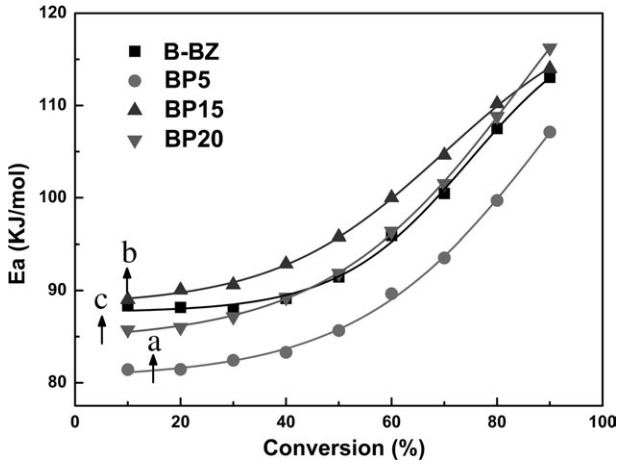

Figure 9. Plots of $E\alpha$ versus conversions according to Ozawa's isoconversional method for B-BZ and B-BZ/PEI blends. Symbols: experiment result, lines: fitting results, arrow: the conversion of BP5 (a), BP15 (b), and BP20 (c) at phase-separation point.

the conversion of B-BZ reached 10%, phase separation occurred in BP15 and BP20 system. From then on, the dilution effect in B-BZ/PEI blends systems was highly dependent on the extent of phase separation, but not on the initial PEI content. The serious dilution effect of BP15 system would result in the highest $E\alpha$ values, while extensive phase separation of BP20 system might permit PB-BZ-rich "nodulus" acting similarly as the pure B-BZ resin, just like the micelles in the emulsion whose polymerization was not affected by the external environment, leading to the overlapping of $E\alpha$ values with B-BZ system. This speculation was highly consistent with the results shown in Figure 9.

Extensive phase separation for BP5 system indeed resulted in the lowest $E\alpha$ value among the three B-BZ/PEI blends. Considering the dilution effect of PEI molecules, the $E\alpha$ of BP5 system should not be lower than that of B-BZ system, if no other interactions existed. But the experiment result in Figure 9 showed that the $E\alpha$ values of BP5 system were 5 kJ/mol lower than those of B-BZ resin at the same conversion ($10\% \leq \alpha_{BZ} \leq 90\%$), which on the other hand suggested that the polymerization of B-BZ resin was facilitated in the presence of small amounts of PEI modifiers.

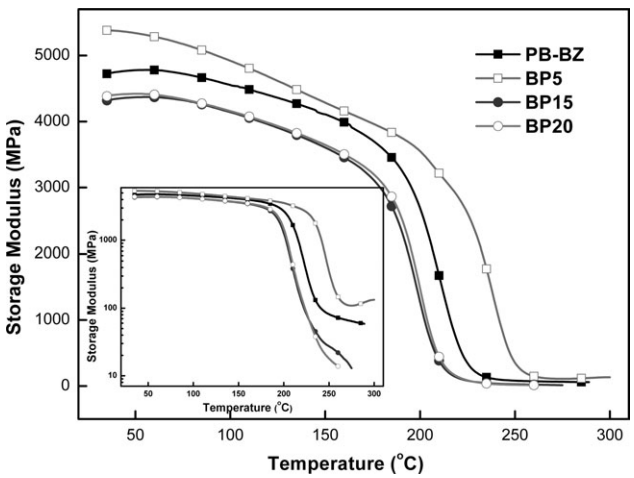

Figure 10. Storage modulus spectra of PB-BZ and PB-BZ/PEI blends.

Table II. Physical Parameters of PB-BZ and PB-BZ/PEI Blending Systems

System	PEI content (wt %)	T_g[a] PEI-rich phase	T_g[a] PBZ-rich phase	ρ[b] (10^3 mol/m^3)
PB-BZ	0		225	5.90
BP5	5	208	254	8.48
BP15	15	214	214	3.46
BP20	20	213	235	2.64
PEI	100	225[c]		

[a]The T_{peak} of tan δ by DMA analysis, [b]Crosslinking density of fully cured system calculated from the statistical theory of rubber elasticity, [c]T_g obtained from tan δ peak according to Figure 5 in Ref. 43.

Dynamic Mechanical Analysis

For TS resins, the changes of the cross-linked network structures can be detected by DMA experiment. Figure 10 clearly showed that the storage modulus (E') of BP5 system was higher than that of PB-BZ system, while the E' of BP15 and BP20 system was slightly lower than that of PB-BZ system over the entire temperature range examined. The storage modulus at low temperature (E_L') is always used to qualitatively characterize the rigidity of the networks. The higher the E_L' value, the higher the rigidity of the network. So, BP5 system had a more rigid structure than PB-BZ, while BP15 and BP20 system had a relative flexible one.

From the rubber elastic theory and the experimental storage modulus (Figure 10) in the rubbery region, the crosslinking density of each system could be estimated according to eq. (2)[40]:

$$Er = 3\phi\rho RT \tag{2}$$

where ø is a front factor, which is unity for ideal rubbers, ρ is the crosslinking density, R is the gas constant, and E_r is the storage modulus at temperature T (T_g + 50 K). This equation has been used in many TS resin systems.[2,41,42] However, this equation is strictly valid only for lightly crosslinked materials and therefore is used only to qualitatively compare the level of crosslinking among the various compositions.[2]

Table II showed that the crosslinking density of PB-BZ/PEI blends decreased with increasing the content of PEI, for the PEI used here was nonreactive. However, it was surprised to find that the crosslinking density of BP5 system (8.48×10^3 mol/m^3) was much higher than that of PB-BZ (5.90×10^3 mol/m^3) system. This was consistent with the $E\alpha$ results mentioned earlier that small amounts of PEI could improve the polymerization extent of PB-BZ. According to the $E\alpha$ results of BP20 system, the crosslinking density of BP20 system should not be lower than that of pure PB-BZ system, but the calculated values were inconsistent, which would be interpreted subsequently.

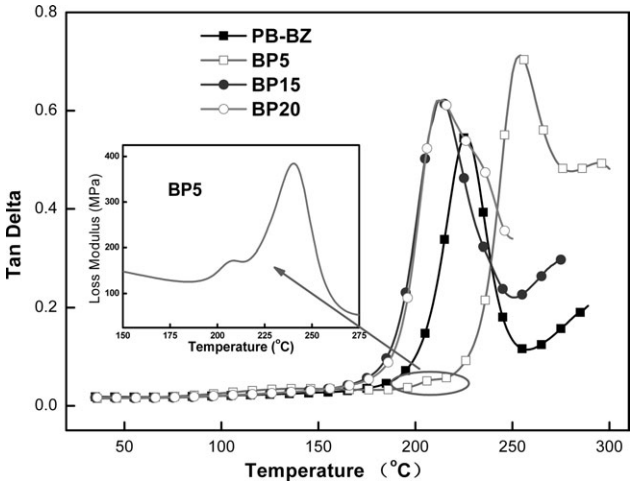

Figure 11. Tan δ spectra of PB-BZ and PB-BZ/PEI blends. (Inset: the loss modulus of BP5 vs. temperature).

From Figure 11, T_g for each system can be got from the temperature corresponding to the peak tan δ. Two relaxation peaks were observed in BP5 and BP20 systems, while only a broad one was obtained in BP15 system. Girard-Reydet et al.[43] believed that the main peak corresponded to the relaxation behavior of matrix phase, and the relative smaller one corresponded to the relaxation behavior of dispersed phase. Combining with the SEM result, the T_g of each phase for PB-BZ/PEI blends was concluded in Table II.

As shown in Table II, the T_g of PEI-rich phase, which was almost independent of the PEI content and phase morphologies, was slightly lower than that of pure PB-BZ and PEI (225°C).[17,43] The decrease of T_g of PEI-rich phase might be attributed to the plasticization of residual PB-BZ resin with low-molecular weight in PEI-rich phase.[17,39]

One interesting thing was that, in BP5 system, the main peak at 254°C attributed to the T_g of PB-BZ matrix phases was 29°C higher than that of single PB-BZ and PEI (225°C). Takeichi et al.[44,45] found that the T_gs values of B-BZ/polyimide polymer alloys remarkably increased as the content of polyimide increased due to the higher T_g of polyimide than that of PB-BZ and the formation of AB cross-linked network structures. In our systems, PEI was nonreactive, and the T_gs of PB-BZ and PEI were equal. So, the increase of T_g of PB-BZ-rich phases should be mainly contributed to the change of PB-BZ network structures. According to the crosslinking density and storage modulus results of BP5 system, the introduction of PEI not only increased the polymerization extent, but also enhanced the rigidity of PB-BZ networks. That is why BP5 system has the highest T_g.

Extensive phase separation was reported to be a precondition for good properties.[17] For BP15 system, serious dilution effect caused by poor phase separation indeed resulted in the low T_g of PB-BZ-rich phase.[15,16,46] Another interesting thing is that, in BP20 system, the shoulder peak at 235°C corresponding to the T_g of PB-BZ-rich phase was 10°C higher than that of single PB-BZ and PEI system. According to the results of storage modulus, BP20 system has a less rigid structure than PB-BZ, and so the higher T_g of BP20 system should be attributed to the increase of polymerization extent of PB-BZ-rich phase. This result was inconsistent with the crosslinking density result of BP20 system (Table II), which could be explained by the fact that the crosslinking density obtained by DMA measurement associated with the crosslinking density of BP20 system, but not associated with the crosslinking density of single PB-BZ-rich phase. Therefore, it can be concluded that the polymerization of B-BZ resin on the incorporation of PEI modifiers does in fact undergo a relatively complete network development. And increasing the polymerization extent is significant to further improve the properties of PB-BZ.

CONCLUSION

By varying the weight fraction of PEI, sea-island structure, dual phase structure, and phase inversion structure were observed in PBZ blends with 5, 15, and 20 wt % of PEI, respectively. Phase separation took place at the early stage of the curing reaction, which effectively reduced the dilution effect of PEI. From the investigation of the morphology evolution process, relatively higher extent of phase separation was obtained in PB-BZ blends with 5 and 20 wt % of PEI, while poor phase separation was observed in PB-BZ blends with 15 wt % of PEI. H-bonds between PEI and PB-BZ existed during the whole curing process, although weakened with phase separation. The exchange of hydrogen bonds between PEI and PB-BZ with the native hydrogen bonds of PB-BZ indeed had a positive effect on improving the polymerization extent of BZ resin. As a result, the crosslinking density of PB-BZ-rich phases in extensive phase separation systems was greatly enhanced, leading to the T_g of PB-BZ-rich phase increased from 225 to 254°C.

ACKNOWLEDGMENTS

Supports for this project were provided by the National Natural Science Foundation of China (Project No. 50873062 and 21104048) and Doctoral Fund of Ministry of Education of China (Project No. 20090181110030).

REFERENCES

1. Ning, X.; Ishida, H. *J. Polym. Sci., Part A: Polym. Chem.* **1994,** *32*, 1121.
2. Ishida, H.; Allen, D. *J. Polymer* **1996,** *37*, 4487.
3. Wirasate, S.; Dhumrongvaraporn, S.; Allen, D. J.; Ishida, H. *J. Appl. Polym. Sci.* **1998,** *70*, 1299.
4. Ning, X.; Ishida, H. *J. Polym. Sci., Part B: Polym. Phys.* **1994,** *32*, 921.
5. Ishida, H.; Allen, D. J. *J. Polym. Sci., Part B: Polym. Phys.* **1996,** *34*, 1019.
6. Kim, H.-D.; Ishida, H. *J. Phys. Chem. A* **2002,** *106*, 3271.
7. Shen, S. B.; Ishida, H. *J. Polym. Sci., Part B: Polym. Phys.* **1999,** *37*, 3257.
8. Su, Y. C.; Chang, F. C. *Polymer* **2003,** *44*, 7989.
9. Ishida, H.; Low, H. Y. *Macromolecules* **1997,** *30*, 1099.

10. Wang, C. F.; Su, Y. C.; Kuo, S. W.; Huang, C. F.; Sheen, Y. C.; Chang, F. C. *Angew. Chem. Int. Ed.* **2006,** *45*, 2248.
11. Schnell, I.; Brown, S. P.; Low, H. Y.; Ishida, H.; Spiess, H. W. *J. Am. Chem. Soc.* **1998,** *120*, 11784.
12. Ishida, H.; Lee, Y. H. *J. Polym. Sci., Part B: Polym. Phys.* **2001,** *39*, 736.
13. Ishida, H.; Lee, Y. H. *Polymer* **2001,** *42*, 6971.
14. Bonnet, A.; Lestriez, B.; Pascault, J. P.; Sautereau, H. *J. Polym. Sci., Part B: Polym. Phys.* **2001,** *39*, 363.
15. Varley, R. J.; Hodgkin, J. H.; Hawthorne, D. G.; Simon, G. P.; McCulloch, D. *Polymer* **2001,** *41*, 3425.
16. MacKinnon, A. J.; Jenkins, S. D.; McGrail, P. T.; Pethrick, R. A. *Macromolecules* **1992,** *25*, 3492.
17. Bucknall, C. B.; Gilbert, A. H. *Polymer* **1989,** *30*, 213.
18. Gan, W. J.; Yu, Y. F.; Wang, M. H.; Tao, Q. S.; Li, S. *J. Macromolecules* **2003,** *36*, 7746.
19. Girard-Reydet, E.; Sautereau, H.; Pascault, J. P.; Keates, P.; Navard, P.; Thollet, G.; Vigier, G. *Polymer* **1998,** *39*, 2269.
20. Bonnet, A.; Pascault, J. P.; Sautereau, H.; Camberlin, Y. *Macromolecules* **1999,** *32*, 8524.
21. Williams, R. J. J.; Rozenberg, B. A.; Pascault, J. P. *Adv. Polym. Sci.* **1997,** *128*, 95.
22. Bonnet, A.; Pascault, J. P.; Sautereau, H.; Taha, M.; Camberlin, Y. *Macromolecules* **1999,** *32*, 8517.
23. Flory, P. J. Principles of Polymer Chemistry; Cornell University Press: New York, **1953; p 464, 576.**
24. Small, P. A. *J. Appl. Chem.* **1953,** *3*, 71.
25. Xiang, H.; Ling, H.; Wang, J.; Song, L.; Gu, Y. *Polym. Compos.* **2005,** *26*, 563.
26. Blanco, I.; Cicala, G.; Motta, O.; Recca, A. *J. Appl. Polym. Sci.* **2004,** *94*, 361.
27. Cicala, G.; Spina, L. R.; Recca, A.; Sturiale, S. *J. Appl. Polym. Sci.* **2006,** *101*, 250.
28. Chen, J. L.; Chang, F. C. *Macromolecules* **1999,** *32*, 5348.
29. Oyanguren, P. A.; Galante, M. J.; Andromaque, K.; Frontini, P. M.; Williams, R. J. *J. Polymer* **1999,** *40*, 5249.
30. Clarke, N.; McLeish, T. C. B.; Jenkins, S. D. *Macromolecules* **1995,** *28*, 4650.
31. Kumar, K. S. S.; Nair, C. P. R.; Sadhana, R.; Ninan, K. N. *Eur. Polym. J.* **2007,** *43*, 5084.
32. Zheng, S. X.; Lü, H.; Guo, Q. P. *Macromol. Chem. Phys.* **2004,** *205*, 1547.
33. Leung, L.; Williams, D. J.; Karasz, F. E.; MacKnight, W. *J. Polym. Bull.* **1986,** *16*, 457.
34. Guerra, G.; Choe, S.; Williams, D. J.; Karasz, F. E.; MacKnight, W. *J. Macromolecules* **1988,** *21*, 231.
35. Low, H. Y.; Ishida, H. *Polym. Degrad. Stab.* **2006,** *91*, 805.
36. Serra, R.; Sempere, J.; Nomen, R. *Therm. Acta* **1998,** *316*, 37.
37. Ishida, H.; Lee, Y. H. *J. Appl. Polym. Sci.* **2001,** *81*, 1021.
38. Pillai, J. P.; Thomas, S. *J. Macromol. Sci., Part A: Pure Appl. Chem.* **2011,** *48*, 751.
39. Francis, B.; Poel, G. V.; Posada, F.; Groeninckx, G.; Rao, V. L.; Ramaswamy, R.; Thoms, S. *Polymer* **2003,** *44*, 3687.
40. Bower, D. I. An Introduction to Polymer Physics; Cambridge University Press: New York, **2002;** Chapter 6, p 181.
41. Shen, S. B.; Ishida, H. *J. Appl. Polym. Sci.* **1996,** *61*, 1595.
42. Musto, P.; Abbate, M.; Ragosta, G.; Scarinzi, G. *Polymer* **2007,** *48*, 3703.
43. Girard-Reydet, E.; Vicard, V.; Pascault, J. P.; Sautereau, H. *J. Appl. Polym. Sci.* **1997,** *65*, 2433.
44. Takeichi, T.; Agag, T.; Zeidam, R. *J. Polym. Sci., Part A: Polym. Chem.* **2001,** *39*, 2633.
45. Takeichi, T.; Guo, Y.; Rimdusit, S. *Polymer* **2005,** *46*, 4909.
46. Raju, T.; Ding, Y. M.; He, Y. L.; Yang, L.; Paula, M.; Yang, W. M.; Tibor, C.; Sabu, T. *Polymer* **2008,** *49*, 278.